PCCP

Accepted Manuscript

ROYAL SOCIETY OF CHEMISTRY

www.rsc.org/pccp

A new interpretation of SAXS peaks in sulfonated poly(ether ether ketone) (sPEEK) membranes for fuel cell

H. Mendil-Jakani*, I. Zamanillo Lopez, P. M. Legrand, V. H. Mareau and L. Gonon

Structure et Propriétés d'Architectures Moléculaires, UMR 5819 SPrAM (CEA-CNRS-UJF), CEA-Grenoble, 17, rue des Martyrs, 38054 Grenoble, Cedex 9, France.

*corresponding author: hakima.mendil-jakani@cea.fr

The structure of a commercial sulfonated poly(ether ether ketone) (sPEEK) membrane was analyzed by Small-Angle X-Ray Scattering (SAXS) for different water uptakes obtained after immersion in liquid water at various temperatures. For low membrane swelling, the SAXS profile displays only a wide-angle peak in the 0.2-0.3$Å^{-1}$ region. As the membrane swells, two supplementary correlation peaks arise and shift towards small angles which is the signature of a structural evolution of the membrane, whereas the wide angle peak remains stable. The SAXS spectra of sPEEK membranes can thus display simultaneously three correlation peaks. Therefore we propose a new interpretation of these SAXS spectra which conclude that the two small angles peaks are attributed to the so-called matrix and ionomer peaks and the wide-angle peak is ascribed to the mean separation distance between sulfonic acid groups grafted onto the polymer backbone. This peak attribution implies that the sPEEK nano-phase separation is triggered by an immersion in hot water (ionomer peak apparition). Our new peak attribution was confirmed by studying the impact of temperature, electron density contrast and ionic exchange capacity.

Keywords: SAXS, sPEEK membrane, fuel cell, nanostructuration, contrast variation, ionic exchange capacity

1 Introduction

Hydrogen fuel cells based on proton exchange membrane are considered as a promising power system for the next generation of electric vehicles operating without emission of any greenhouse gas. The polymer membrane sandwiched between electrodes acts as a proton conductor and a gas separator. The benchmark materials are perfluorosulfonated ionomers (Nafion® type) due to their outstanding performances and stability for fuel cell application. The extremely hydrophobic perfluorinated backbone is grafted by perfluorovinyl ether units that are terminated by hydrophilic sulfonic acid groups. This gives rise to a well-defined nano-separated morphology with well-connected hydrophilic domains which strongly enhance the proton conductivity[1, 2]. In order to develop better membranes for PEMFC, it is therefore of prime importance to understand the relationship between the membrane microstructure and its proton transport properties. The microstructure of Nafion® has been extensively studied by Small Angle Neutron Scattering (SANS) and Small Angle X-Ray Scattering (SAXS) but is still the subject of active debates[3, 4]. The SANS and SAXS spectra display the so-called ionomer peak at a "q" position that depends on the level of membrane hydration ($0.1<q<0.2$ Å^{-1}). This correlation peak is the signature of the ionomer membrane microstructure and originates from its hydrophobic/hydrophilic nano-phase separation[5]. Its "q" position is associated to a Bragg spacing "$d=2\pi/q$" which is the mean separation distance between interconnected ionic domains. Subsequent to the pioneering Gierke model of Nafion® which described the membrane as a network of water clusters connected by channels[6], many other structural models have emerged to interpret the swelling behavior of perfluorosulfonated membranes. Recently, a model describing Nafion® as a matrix of embedded parallel cylindrical water nanochannels and crystallites was developed by Schmidt-Rohr *et al.*[7], contrasting with the previously proposed fibrilar model of Rubatat *et al.* based on

charged polymer ribbons surrounded by a water continuum[8, 9]. These active debates demonstrate the difficulty to get a clear picture of the morphology of Nafion® membrane.

As already stressed, Nafion® type ionomers are benchmark materials for PEMFC membranes. However, in addition to a high cost, these perfluorinated polymers exhibit, at elevated temperatures, both weak mechanical properties and strong dehydration. These are major drawbacks that prohibit a large-scale application of this type of fuel cell since higher running temperatures (T>100°C) are expected in order to reach faster electrochemical reaction and increase tolerance of the catalyst to CO poisoning.

Sulfonated hydrocarbon-membranes based on a rigid poly-aromatic backbone such as sulfonated poly(ether ether ketone) (sPEEK) seem to be promising candidates[10] from a thermomechanical point of view as they show higher mechanical transition temperatures[11]. This chemistry is also interesting due to the lower cost and finally the lower environmental impact as compared to fluorine chemistry. Compared to Nafion® type ionomers, the phase separation between hydrophilic and hydrophobic domains is much less pronounced for sPEEK (both the lower hydrophobicity of sPEEK polymer backbone and the lower acid strength of the sulfonic acid groups induce a phase separation driving force much lower than for Nafion®[1]) which explains in part the highly reduced gas crossover compared to PFSA membranes[12]. The literature on sPEEK microstructure is scarce and quite recent[1, 13-17]. In addition the possibility to design sPEEK membranes with various degrees of sulfonation (DS), to use different casting solvents and membrane cleaning procedures gives rise to a large span of SAXS spectra with characteristic peaks located at different scattering ranges. A clear picture of the sPEEK membrane morphology can thus hardly emerge.

We have studied the impact of the swelling state of sPEEK membranes on the SAXS spectra. These experiences have outlined a much more complex scattering pattern than reported in the literature: **three correlation peaks have been identified simultaneously**. We propose here a

new interpretation of sPEEK SAXS spectra, including a **new peak attribution**. The effects of **immersion water temperature**, **electron density contrast**, **ionic exchange capacity** and **membrane crystallinity** on the scattering profiles confirm this new interpretation. This work also demonstrates that the sPEEK nanostructuration is triggered by immersion in water at high temperatures, which is a key parameter to optimize sPEEK membrane performances.

2 Experimental

The studied sPEEK membranes, which chemical repeat unit is represented on Figure 1, were provided from Fumatech® (Fumapem®) with equivalent weights EW (mass of the dry polymer per mole of ionic group SO_3) ranging from 330 to 840 g/eq.

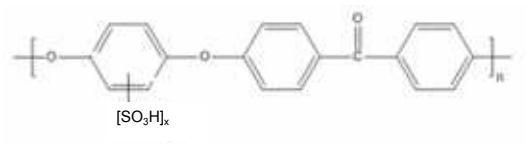

Fig. 1 Chemical repeat unit of sPEEK

sPEEK membranes were obtained by the sulfonation of the hydrophobic PEEK. The substitution takes place preferentially in one of the four positions of the aromatic rings located between the ether groups (first type substitution)[18]. A sulfonation degree over 100% can be obtained after the completion of this first type substitution[19]. The second type substitution occurs by the sulfonation of the aromatic rings located at each side of the ketone group, at high temperatures and/or over long time of reaction between PEEK and sulfuric acid due to the electron withdrawing effect of the sulfonated group which reduces the reactivity of the adjacent aromatic ring[19].

Table 1 lists the corresponding ionic exchange capacity (IEC) and degree of sulfonation (DS) with

$$IEC=1000/EW \quad (1)$$

and

$$DS = \frac{M_p}{EW - M_{SO_3H}} \quad (2)$$

where M_p and M_{SO_3H} the molecular weight of a non-sulfonated unit (288 g/mol) and a SO_3H group (81 g/mol) respectively.

Table 1. sPEEK equivalent weight (EW), ionic exchange capacity (IEC) and degree of sulfonation (DS)

Material reference	EW (g/eq)	IEC (meq/g)	DS%
sPEEK(3)	330	3.0	115
sPEEK(1.8)	550	1.8	61
sPEEK(1.6)	630	1.6	52
sPEEK(1.33)	750	1.33	43
sPEEK(1.2)	840	1.2	38

The membranes will be labeled sPEEK(IEC). The as received sPEEK membranes were reacidified before use (4h acidification in a molar sulfuric acidic solution at room temperature, followed by triple rinsing with pure water).

2.1 Membrane treatment and conditioning for SAXS analysis.

Membrane swelling

sPEEK(1.33) was soaked in pure liquid water at different temperatures (20, 35, 60, 80, 100, 120°C) for a same immersion time of 96h (duration for a water uptake equilibrium). For 120°C, the membrane was swollen in a water filled autoclave. The other membranes were analyzed after 96h of immersion in liquid water at 20 and 80°C.

Ionic exchange

After the membrane swelling, classic ionic exchange with Cs^+ is realized by immersing the membrane in a large amount of a 0.1 M solution of CsCl salt during 4h followed by thorough water rinsing (three times). This Cs^+ ionic exchange enhances the

electron density contrast between the hydrocarbon sPEEK polymer matrix and the ionic domains.

sPEEK(1.33) in K^+ and H^+ forms were obtained following the previous protocol with immersion in KCl, 1M and H_2SO_4, 1M solution respectively, followed by thorough rinsing.

Conditioning

The samples were cut into a 7 mm diameter disc and they were mounted in the SAXS cells with a drop of water. The sealing was ensured by using O-rings on Kapton® foils windows.

Membrane water uptake (λ, ϕ_p)

The membranes were cut into rectangular pieces (6×3 cm²) and immersed in liquid water at a given temperature (from 20 to 120°C) during 96h. To obtain the wet weight (m_{wet}), the excess water was gently removed with filter paper before weighing the swollen membranes. The dry weight (m_{dry}) was measured after drying under vacuum at room temperature overnight. The water uptake, defined with λ as the number of water molecules per ionic site, was calculated as:

$$\lambda = \frac{EW}{M_{H_2O}} \cdot \frac{(m_{wet} - m_{dry})}{m_{dry}} \quad (1)$$

Where M_{H2O} is the molar mass of water and EW the polymer equivalent weight.

The polymer volume fraction in the membrane is defined as:

$$\Phi_p = 1 - \frac{\lambda \cdot d_p / d_e}{\lambda \cdot d_p / d_e + EW / M_{H_2O}} \quad (2)$$

where d_p is the polymer density (1.4 g.cm^{-3}), d_e the water density (1 g.cm^{-3}).

2.2 SAXS-WAXS experiments

SAXS spectra were recorded on ID2 High Brilliance Beamline and D2AM-CRG beamline at the ESRF (Grenoble). The X-Ray scattering intensity was measured as a function of the scattering vector "q" defined as $q=4\pi/\lambda.\sin(\theta)$ where 2θ is the scattering angle and λ the wavelength of the incident X-Ray beam. The Bragg spacing "d" is related to "q" as: $d=2\pi/q$. Measurements were carried out at $\lambda=1$ Å with a sample-to-detector (a 2D-CCD camera) distance of D=1 m (ID2) and $\lambda=0.77$ Å with D=0.75 m (D2AM). These configurations, used with centered X-Ray beam with respect to the sample, allowed covering an extended "q" range from 10^{-2} to 0.4 $Å^{-1}$. The 2D-scattering patterns were isotropic, therefore the 1D scattering curves (Intensity=f(q)) were obtained after integration over all directions.

Complementary SAXS spectra were recorded with a homemade apparatus at CEA-Grenoble/INAC, using a CuK_α radiation ($\lambda=1.5418$ Å) source generated by a rotating anode. Two "sample to detector" distances of 1.50 m and 0.80 m with an off-centred configuration were chosen and allow covering an extended angular "q" range from 0.01 to 0.5 $Å^{-1}$. Two pieces of water swollen membrane were superimposable and were placed in a SAXS cell between two Kapton® foils. Usual corrections were applied to the data for background subtraction and normalization[20].

Wide-Angle X-Ray Diffraction (WAXD) patterns were recorded with a Panalytical X'Pert diffractometer equipped with a Copper X-ray tube ($\lambda K_{\alpha 1}=1.5418$ Å) delivering a linear beam and with a 1D X'Celerator detector (CEA-Grenoble/INAC). A 0.5° divergence slit was used on the primary path with a set of anti-scattering slits before and after the sample. Axial divergence was limited by 0.02 rad Soller slits. The measurements were performed in $\theta/2\theta$ transmission geometry. The data were recorded for 2θ ranging from 7° to 50° (0.5 to 3.4 $Å^{-1}$) with a step of 0.04° and a time per step of 300s. The samples were equilibrated at room temperature and relative humidity (20°C, 45% RH).

3 Results and discussion

3.1 Identification of the swelling impact on the membrane microstructure.

We studied the structure of sPEEK(1.33) membranes swollen in liquid water for 96h at 20, 35, 60, 80, 100 and 120°C. Figure 2 displays the SAXS spectra of these membranes in Cs^+ form conditioned in liquid water (only few drops to prevent membrane drying during experiment) at room temperature.

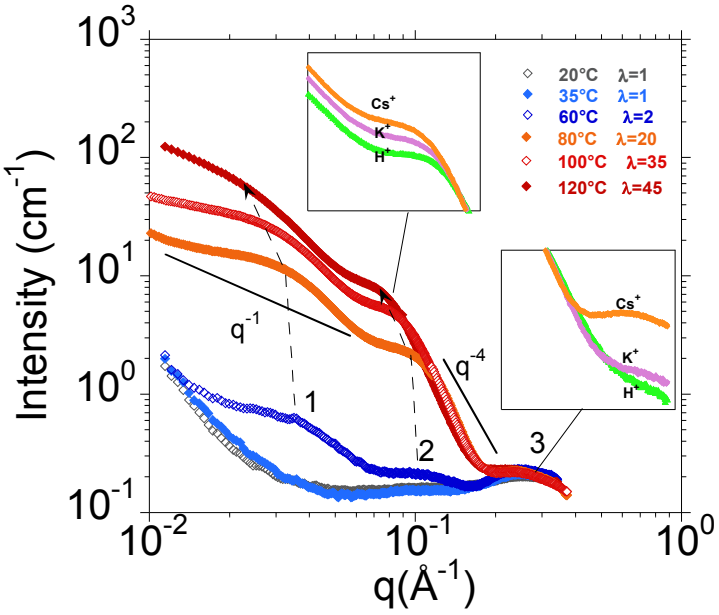

Fig. 2 Log-log SAXS profiles of water swollen sPEEK(1.33) membranes in Cs^+ form at room temperature after 96h of immersion in liquid water at 20(◇), 35(◆), 60(◇), 80(◆), 100 (◇) and 120°C(◆). The left and right insets compare the SAXS profiles, at 80°C, in the peak 2 and peak 3 regions respectively, for different monovalent counter ions: Cs^+, K^+ and H^+. The spectra were recorded at ID2 and D2AM ESRF beamlines.

For immersion temperatures below 60°C (very low swelling, λ=2), it is observed that the scattering profiles are superimposable. These profiles exhibit an intense small-angle upturn, classically observed for ionomers[21] followed by a rather flat "q" range at intermediate scattering vectors (0.04-0.15 Å^{-1}) and terminated by a low intensity and broad peak at wide angle (large "q", labeled peak "3") at about 0.25 Å^{-1}. It is associated to a characteristic distance d_3 of $2\pi/q_3 \sim 25$ Å. For higher immersion temperatures, the membrane swelling dramatically increases (λ≥20) and one can observe the emergence of two additional peaks at

smaller angles, labelled peaks "1" and "2". At 60°C, they are located at about q_1~0.037 $Å^{-1}$ and q_2~0.1 $Å^{-1}$ and are associated to characteristic Bragg distances d_1 and d_2 of $2\pi/q_1$~170 Å and $2\pi/q_2$~63 Å respectively. **It is important to note that these three peaks are evidenced simultaneously on SAXS spectra of sPEEK membranes.**

For sPEEK(1.33), the evolution of the scattering profile with the swelling temperature is observed to be a two-step process. First step is an abrupt departure of the scattered intensity observed from 60°C to 80°C without significant peak shifting. In a second step, for temperatures above 80°C, peaks "1" and "2" shift towards smaller angles and their intensity increases.

From 80°C, it is observed that peak "2" is followed by a "q^{-4}" behavior (Porod's law) in the wide angle region. This is the typical signature of a sharp interface between two phases, certainly the hydrophobic and the hydrophilic ones. Peak "2" is therefore assigned to the so-called **ionomer peak** as it presents similar features as perfluorosulfonated membranes upon swelling [6, 22]: **a small angle peak shifting together with an increase in intensity and a q^{-4} behavior at the nanometer scale.**

From the observation of a macroscopic swelling, provided that the membrane is soaked in hot water, together with the appearance of an ionomer peak (fingerprint of the nano phase separation), we understand that this immersion in water at elevated temperatures (from 60°C) allows sufficient molecular mobility to improve the self-assembly (hydrophilic-hydrophobic) which results in a better nanostructuration of the membrane and provides a **well-defined interface** between hydrophilic and hydrophobic phases (from 80°C: Porod's law). In other words, the ionic domains grow, up to making a continuous phase, and their separation with the rest of the membrane becomes sharper. It should be noted that this temperature-dependant nanostructuration contrasts drastically from what is known for Nafion® for which a ionomer peak, together with a "q^{-4}" behavior are observed from the very first step of hydration

obtained at room temperature (low λ values, typically 2)[8]: Nafion® is intrinsically nano phase separated.

This very good nano phase separation observed for Nafion® explains why its conductivity is 30 times better than that of sPEEK at 100°C and 35% RH as observed by Alberti *et al*[23]. However the same authors have found that both membranes exhibit comparable conductivity at 160°C and 75% RH, a spectacular improvement for sPEEK that they attribute to a better ability of the sPEEK membrane to retain water. This improvement can be explained by the nanostructuration process that we identified for sPEEK.

We plotted in Figure 3 the characteristic distance between the scattering entities ($d_{iono}=2\pi/q_{iono}$ with "iono" standing for ionomer) as a function of the membrane swelling (the polymer volume fraction Φ_p of the swollen membranes), for both Nafion®(117) and the nanostructured sPEEK(1.33).

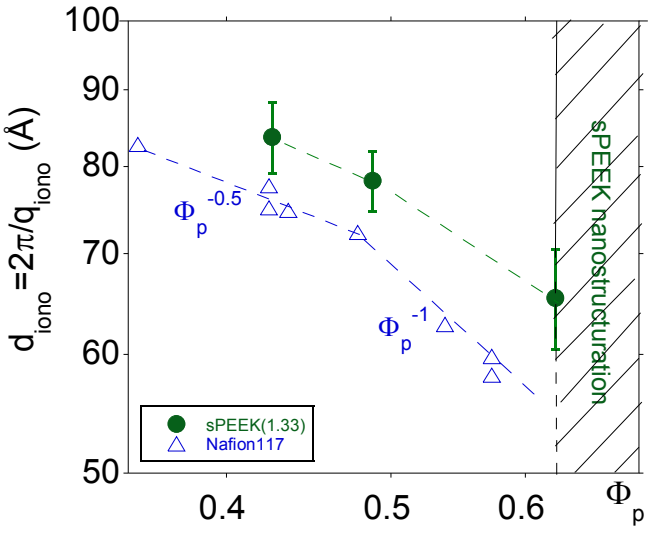

Fig. 3 Log-log evolution of the characteristic distance $d_{iono}=2\pi/q_{iono}$ as a function of the polymer volume fraction Φ_p for the nanostructured sPEEK(1.33) and Nafion® 117 (data extracted from ref[8]). The dotted line for sPEEK(1.33) is a guide for the eyes.

In Figure 3, it should be first stressed that we dispose of very limited SAXS data for sPEEK(1.33). However, it appears reasonable to compare the swelling behavior of

sPEEK(1.33) and Nafion® for two main reasons. First, it was recently evidenced that the scattering entities for sPEEK ionomer dispersions are ribbon-like polymer particles as for Nafion®[17]; second, flat morphologies seem to be a general feature for most dissociated ionomers[4], and similar dilution laws are therefore expected. Then, we can observe that the plot $d_{iono}=f(\Phi_p)$ of sPEEK(1.33) seems to exhibit a discontinuity, similarly to Nafion®. Indeed, for Nafion®117, the Φ_p^{-1} behavior observed at high Φ_p values, down to ~47%[24], was associated to the dilution of flat objects as ribbons[7]. For higher swellings, (lower Φ_p values) a $\Phi_p^{-0.5}$ dilution law was associated to the dilution of rod-like objects like cylinders. Finally, it appears that once sPEEK(1.33) is nanostructured (for Φ_p values lower than the hatched area in Fig.3 as from 80°C a q^{-4} Porod's law is observed), it exhibits similar swelling behaviors as Nafion®117. In brief, the main difference between both ionomers in terms of swelling behaviour is that Nafion® is intrinsically nanostructured while sPEEK requires a hydrothermal treatment to reach a well-defined nano-phase separation.

Another similarity between Nafion®117 and sPEEK(1.33) is the observation on Fig 2. of a peak located at smaller angles than the ionomer peak (peak 1), less pronounced and observed above a q^{-1} slope[8]. This peak displays similar features as the so-called matrix peak (and will be labelled as such), usually understood as originating from inter-crystallite interferences [25].

In contrast with both the ionomer and the matrix peaks, the wide angle peak "3" intensity and position are quite insensitive to the thermally induced nanostructuration. Indeed peak "3" position is about 0.256 $Å^{-1}$ from 25°C to 60°C and about 0.25 $Å^{-1}$ from 80°C up to 120°C. The observation of **peak "3" remaining stable during the membrane nanostructuration**, strongly suggest that this peak is likely to be related to an **intramolecular correlation distance, like the mean separation distance between sulfonated units along the rigid polymer backbone. Therefore this peak will be hereafter abbreviated as "SO_3" peak.** The broadness of the peak reflects the fact that the sulfonated

units are not uniformly distributed along the polymer backbone. This statistical distribution results from the chemical process used to prepare the materials (dissolution time, withdrawing effect of the SO_3H groups grafted onto the aromatic ring).

One could then wonder why this SO_3 peak has never been observed for perfluorosulfonated polymeric systems[6, 8, 22]. This can be understood by comparing the molecular architecture of Nafion® and sPEEK. For Nafion®, SO_3H groups are located at the extremity of highly flexible side chains, grafted onto the Teflon®-like polymer backbone. In contrast, for sPEEK, SO_3H groups are directly grafted onto the aromatic rings of the highly rigid sPEEK backbone. Both Nafion® architecture and its high side chain mobility prevent the observation of the wide angle peak characteristic of the distance between SO_3 groups. It should be noted that the same conclusions are true for the aromatic polymers developed by Jannasch *et al.*[26] that carry hypersulfonated side chains: no SO_3 peak is observed despite their better nanostructuration. One should also wonder why for the aromatic ionomers with precisely sequenced sulfonated moieties *along* the polymer backbone developed by Jannasch *et al.*[27] no such SO_3 peak was observed. In that case, on the one hand the distance between SO_3 groups located in the same hydrophilic blocs is so short that their corresponding peak would be located at wider angles, not explored in their work. On the other hand the distance between SO_3 groups separated by long hydrophobic sequences is so large that their corresponding peak would be found at a similar scattering range as the ionomer peak. However, these authors can observe a second-order peak that arises from a high level of long-range ordering. This peak cannot be attributed to the SO_3 peak. Indeed both the ionomer and second order peaks shift towards smaller angles with increasing IEC[28], whereas the ionomer peak of sPEEK shifts towards smaller angles while its SO_3 peak shifts towards wider angles with IEC (see section 3.2).

Additionally, to the best of our knowledge, for two other membrane types (one sulfonated polyimide (sPI)[29] and one radiation grafted perfluorinated membranes with sulfonated

polystyrene[5]), it was proposed that the wide angle peak, which was observed simultaneously with the ionomer peak, can be attributed to the characteristic distance between sulfonated units within the swollen ionic domains[5, 29]. These previous data on membranes which exhibit some architecture similarities with sPEEK, accredit our wide angle peak attribution.

3.2 Identification of the electron density contrast and IEC impact on the membrane microstructure.

After this preliminary attribution, we will now ascertain our analysis by investigating first the impact of the electron density contrast on the SAXS profiles, second the impact of the IEC.

The insets of figure 2 display, for the ionomer peak and the SO_3 peak regions, the SAXS profiles of water swollen sPEEK(1.33) membranes after immersion in liquid water at 80°C for 96h, followed by ionic exchange with 3 different monovalent counter-ions: Cs^+, K^+ and H^+ with their atomic number Z following: $Cs^+ > K^+ > H^+$(from the higher to the lower atomic number Z) in order to modulate the electron density contrast. The ionomer peak inset shows that this peak position is almost independent of the monovalent counter-ion (slight peak shift is classically observed for ionomers[9, 17]) while its intensity increases with the atomic number Z as a result of an increased contrast. These features confirm our ionomer peak attribution[30, 31]. The SO_3 peak inset shows that this peak position is also independent of the counter-ion atomic number (intrachain correlations) but the effect on its intensity is much more pronounced than for the ionomer peak: decreasing Z strongly lowers the peak intensity and is no longer visible in the H^+ form. This observation strengthens the attribution of the wide angle peak to a structural peak associated to interference effects inside the swollen ionic domains[32].

Figures 4A and 4B display, for different IEC, the SAXS profiles of Cs^+ exchanged sPEEK membranes (liquid water conditioning) after 96h of immersion at 20°C and 80°C. These two temperatures were chosen based on what was observed for sPEEK(1.33): before

(20°C) and after (80°C) nanostructuration. Figures 4C and 4D report the mean separation distance between, respectively, sulfonated units d_{SO3} (SO_3 peak) and ionic domains d_{iono} (ionomer peak) as a function of IEC, at both 20°C and 80°C for 4C and at 80°C only for 4D.

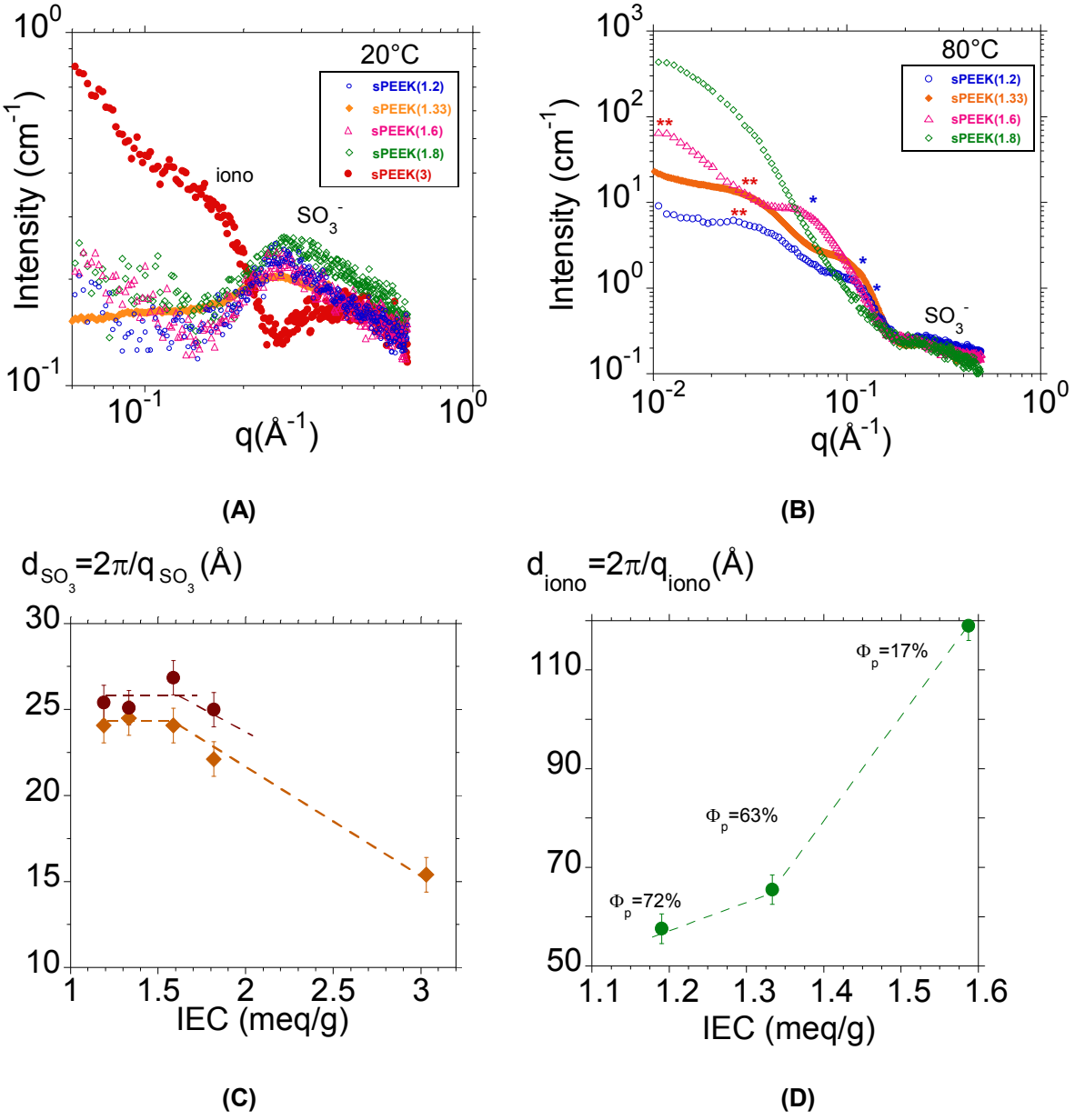

Fig. 4. (A) Log-log SAXS profiles (recorded at ID2 beamline at ESRF and INAC/CEA Grenoble) of Cs^+ exchanged sPEEK. IEC: 1.2 (○), 1.33 (◆), 1.6 (△), 1.8 (◇) and 3 (●). Membranes were conditioned in liquid water at room temperature after 96h of immersion at 20°C **(B)** and at 80°C. One blue star (*) and two red stars (**) show the peak positions of the ionomer and matrix peaks respectively. **(C)** Mean separation distance between sulfonated units (SO_3 peak) ($d_{SO3}=2\pi/q_{SO3}$) as a function of the IEC (meq/g) for 96h of immersion in liquid water at 20°C(◆) and 80°C(●). **(D)** Mean separation distance between ionic domains (ionomer peak) ($d_{iono}=2\pi/q_{iono}$) as a function of the IEC (meq/g) for 96h of immersion in liquid water at 80°C. The dotted lines are guides for the eyes.

At 20°C, it was observed on Fig. 4A (lower signal/noise ratio for sPEEK(1.2), (1.6), (1.8) and (3) obtained from our lab SAXS spectrometer compared to sPEEK(1.33) obtained from synchrotron) that only sPEEK(3) displays a ionomer peak located at ~0.177 $Å^{-1}$. In contrast to sPEEK(1.33), sPEEK(3) does not need immersion at higher temperature than 20°C to show a nanostructuration (at 80°C it is water soluble). It was observed that the SO_3 peak position (corresponding distance $d_{SO3}=2\pi/q_{SO3}$) is almost constant at about 0.26 $Å^{-1}$ (24 Å) for IEC ranging from 1.2 to 1.6, then starts shifting towards higher q values with 0.28 $Å^{-1}$ (22 Å) for sPEEK(1.8), up to a strong shift, 0.4 $Å^{-1}$ (16 Å) observed for sPEEK(3). It should be noted that the SO_3 peak of sPEEK(3) is much narrower than SO_3 peaks of lower IEC as a result of a more homogeneous distribution of the sulfonated groups (all the repeat units are sulfonated). For better visualization, d_{SO3} is reported as a function of IEC on Fig 4C. For the low IEC range, the stable position of the SO_3 peak can be explained by the post-sulfonation process used to obtain the studied sPEEK. Indeed this process naturally produces heterogeneous distribution of the SO_3H groups (parts of the sPEEK chains highly sulfonated contrasting with non sulfonated ones) along the polymer backbone for the lower sulfonation extent. In fact the polymer dissolution process results into a distribution of the sulfonation times among polymer chains (not all the chains being solubilized at the same time). For the higher IEC, the strong SO_3 peak shifting results from a decrease of the mean separation distance between sulfonated units along the polymer backbone. This sulfonation of more than one aromatic ring per repeat unit is obtained by the second type substitution[19]. The peak's narrowing therefore results from a sulfonation becoming much more homogeneous. The mean separation distance d_{SO3} (calculated from the bond lengths[33]) for DS=50% is about 27 Å which is in good agreement with the experimental distance of ~25 Å measured for comparable DS.

For each IEC, it is observed that SO_3 peak is located in the same scattering range at 20°C (Fig. 4A) and at 80°C (Fig. 4B), with however a small shift towards slightly smaller angles (higher

distances) at 80°C, as better observed in Fig. 4C. We assume that this evolution with the temperature can be understood as resulting from a slight stress release. Globally d_{SO3} is thus almost unaffected by the nanostructuration (already observed to occur between 60 and 80°C for sPEEK(1.33) in Fig.2, and observed to be achieved at 80°C for sPEEK(1.2), sPEEK(1.33) and sPEEK(1.6) in Fig.4B as the ionomer peak is clearly observed).

The high swelling state of sPEEK(1.8) at 80°C (Φ_p<15%) prevents interference effects between hydrophobic areas and therefore no ionomer peak is observed[8]. sPEEK(3) which was water soluble at 80°C was not measured. As we observed the ionomer peak for different IEC, we can note that when the IEC increases, this peak grows and shifts towards smaller angles (better swelling properties = increased distances between scattering entities as illustrated by Fig.4D). Indeed, even though the glass transition temperature (Tg) increases with IEC[34], water uptake increases also. Therefore, the higher Tg observed for dry membranes with IEC does not hinder the nanostructuration process.

Increasing IEC has also a strong impact on the matrix peak. This peak is clearly observed for both sPEEK(1.2) and (1.33), less pronounced for (1.6), and missing for higher IEC. When observed, this peak shows a clear shift towards smaller angles. As already stated, we attributed this peak to the matrix one in an analogy with perfluorosulfonated membranes[25]. Indeed, for Nafion®, this peak is observed providing that the membrane exhibits crystallinity[25, 35]. We verified that good agreement exists between our matrix peak observation and the sPEEK crystallinity, by performing WAXD experiments. These data are presented in the supplementary information, and clearly show that sPEEK(1.2) and (1.33) exhibit a sharp crystalline peak, sPEEK(1.6) still has some extent of crystallinity, whereas sPEEK with higher IEC is completely amorphous, which confirm our peak attribution, and was expected since the sulfonated units can hinder the sPEEK crystallization.

3.3 Misleading attribution of the sPEEK wide angle peak in the literature

A few studies have focused on the structural characterization of polyaromatic membranes such as sPEEK[1, 36-38]. Generally, only one peak was observed in the scattering spectra and was naturally attributed to the so-called ionomer peak. Thanks to our observation of three simultaneous peaks in the scattering spectra of sPEEK, we understand that a single peak observation can result into misleading interpretation. Indeed there are two possible confusions. First, the SO_3 peak, if alone, can be confused with the ionomer peak if we do not follow its behavior over a large range of swelling. Second, when variations of the experimental conditions lead to the successive observation of the SO_3 peak and then of the ionomer peak (or *vice versa*) it is possible to confuse these successive observations of two distinct peaks, with a single peak shifting (generally attributed to the ionomer peak). For example, Kawaguti *et al*[15], who measured SAXS data for sPEEK swollen in water or ethanol at room temperature, first confuse the wide angle peak (identical q range as our SO_3 peak) of their low IEC sPEEK with the ionomer peak. Then for higher IEC, where their sPEEK membrane exhibits sufficient nanostructuration, they do observe the ionomer peak (identical q range as our ionomer peak), and they unfortunately miss the SO_3 peak located at higher q, due to its much lower intensity, therefore hidden by the logarithmic scale. Another example of this type of confusion is provided by the work of Yang and Mathiram[38] who concluded on opposite microstructural evolution of ionic clusters, when increasing IEC, for sPEEK membranes both dry or swollen in methanol solution at temperatures ranging from 40 to 80°C. Thanks to our peak attribution, we understand that for dry membranes they confuse the SO_3 peak with the ionomer peak, and therefore conclude on a decrease of the ionic clusters distances when increasing IEC which is counterintuitive. The same erroneous interpretation was recently published by Song *et al*[13] for sPEEK membranes swollen in water at room temperature leading to an underestimation of the persistence length of the sPEEK backbone. They found a surprising 9 Å (when the literature gives about 55 Å[39]) which is much lower

than that of a more flexible chain of Nafion® ~30-50 Å[7] . Finally, we understand that in both works they observe, instead, the decrease of the mean separation distance between sulfonic acid groups when increasing IEC, like reported in Fig.4(c).

Recently, it was stated that our attribution [40] of the wide-angle peak (about 0.25 $Å^{-1}$ for sPEEK(1.33)) to the SO_3 peak was wrong[17] based on diverging interpretations, concluding that it "arises obviously from the form factor of the ionic domains". As we observed a clear shift of this peak towards higher q values (smaller distances) for high degree of sulfonation, as this peak intensity decreases when decreasing the atomic number of the counter ion, as we also observe that the extent of ionomer swelling has no, or very little impact on the peak position, there is no doubt that this peak is related to the mean separation distance between SO_3 groups, and cannot be related to the form factor of the ionic domains.

4 Conclusions

By studying the impact of the swelling temperature on the sPEEK nanostructure, we evidenced simultaneously three peaks on SAXS spectra of sPEEK membranes, where two peaks are usually observed for perfluorosulfonated ones. We found that the wider angle peak, which is usually attributed in the sPEEK literature to the ionomer peak or more recently to the form factor of ionic domains, is in fact associated to the mean separation distance between sulfonic acid groups. We also undoubtedly attributed the two other small angle peaks of the nanostructured membrane to the ionomer and the matrix peaks.

This peak attribution was confirmed when studying the impact of the electron density contrast and the impact of the IEC on the peaks positions and intensities. In addition it was observed that the matrix peak of sPEEK was clearly associated to the polymer crystallinity, like for Nafion® (see supplementary information).

This new peak attribution, evidencing the existence of the wide angle SO_3 peak, has a strong impact on previous sPEEK structure SAXS studies.

Thanks to this new attribution of the SAXS peaks, we indeed understood that the immersion of sPEEK in water at elevated temperatures allows molecular rearrangements that nanostructure the membrane and provide a well-defined interface between hydrophilic and hydrophobic phases. sPEEK being to that matter very different from Nafion which is intrinsically nano phase separated.

Then, a good control of this nanostructuration process appears to be mandatory in order to optimize sPEEK membrane fuel cell properties, or as a preliminary step before making any sPEEK hybrid membrane (introduction of nanoparticules or sol-gel networks inside the membrane for example).

Acknowledgments

The authors acknowledge Michael Schuster and Yervant Bohdjalian from Fumatech® for kindly providing sPEEK membranes, the ESRF for the beamtime allocation, Manuel Fernández Martínez (ID2 beamline) and Cyrille Rochas (BM02-D2AM beamline) for their help as local contacts and especially Cyrille for his effort to help us in clarifying some questions. Olivier Diat is also warmly acknowledged for complementary SAXS tests (at ICSM-UMR5257 Bagnols-sur-Cèze, France), for discussions and for his interest in our work. Arnaud de Geyer is thanked for technical help during SAXS experiments (INAC/CEA Grenoble).

References

1. K. D. Kreuer, *Journal of Membrane Science*, 2001, 185, 29-39.
2. K. D. Kreuer, S. J. Paddison, E. Spohr and M. Schuster, *Chemical Reviews*, 2004, 104, 4637-4678.
3. K. A. Mauritz and R. B. Moore, *Chemical Reviews*, 2004, 104, 4535-4585.
4. K. D. Kreuer and G. Portale, *Advanced Functional Materials*, 2013, DOI: 10.1002/adfm.201300376.
5. G. Gebel and O. Diat, *Fuel Cells*, 2005, 5, 261-276.
6. T. D. Gierke, G. E. Munn and F. C. Wilson, *J Polym Sci Pol Phys*, 1981, 19, 1687-1704.
7. K. Schmidt-Rohr and Q. Chen, *Nature Materials*, 2008, 7, 75-83.
8. L. Rubatat, A. L. Rollet, G. Gebel and O. Diat, *Macromolecules*, 2002, 35, 4050-4055.
9. L. Rubatat, G. Gebel and O. Diat, *Macromolecules*, 2004, 37, 7772-7783.
10. M. A. Hickner, H. Ghassemi, Y. S. Kim, B. R. Einsla and J. E. McGrath, *Chemical Reviews*, 2004, 104, 4587-4611.
11. P. X. Xing, G. P. Robertson, M. D. Guiver, S. D. Mikhailenko, K. P. Wang and S. Kaliaguine, *Journal of Membrane Science*, 2004, 229, 95-106.
12. K. D. Kreuer, *Chemistry Materials*, dx.doi.org/10.1021/cm402742u | Chem. Mater.
13. J. M. Song, J. Shin, J. Y. Sohn and Y. C. Nho, *Macromolecular Research*, 2012, 20, 477-483.
14. B. Yang and A. Manthiram, *Electrochemical and Solid State Letters*, 2003, 6, A229-A231.
15. C. A. Kawaguti, K. Dahmouche and A. d. S. Gomes, *Polymer International*, 2011, 61, 82-92.
16. D. X. Luu, E. B. Cho, O. H. Han and D. Kim, *Journal of Physical Chemistry B*, 2009, 113, 12160-12160.
17. G. Gebel, *Macromolecules*, 2013, 46, 6057-6066.
18. X. G. Jin, M. T. Bishop, T. S. Ellis and F. E. Karasz, *British Polymer Journal*, 1985, 17, 4-10.
19. R. Y. M. Huang, P. H. Shao, C. M. Burns and X. Feng, *Journal of Applied Polymer Science*, 2001, 82, 2651-2660.
20. P. Lindner and T. Zemb, *Neutron, X-Rays and light scattering: Introduction to an investigate tool for colloidal and polymeric systems* North Holland-Elsevier, Amsterdam, 1991.
21. Y. S. Ding, S. R. Hubbard, K. O. Hodgson, R. A. Register and S. L. Cooper, *Macromolecules*, 1988, 21, 1698-1703.
22. K. D. Kreuer, M. Schuster, B. Obliers, O. Diat, U. Traub, A. Fuchs, U. Klock, S. J. Paddison and J. Maier, *Journal of Power Sources*, 2008, 178, 499-509.
23. G. Alberti, M. Casciola, L. Massinelli and B. Bauer, *Journal of Membrane Science*, 2001, 185, 73-81.
24. G. Gebel, *Polymer*, 2000, 41, 5829-5838.
25. M. Fujimura, T. Hashimoto and H. Kawai, *Macromolecules*, 1981, 14, 1309-1315.
26. B. Lafitte and P. Jannasch, *Advanced Functional Materials*, 2007, 17, 2823-2834.
27. X. F. Li, F. P. V. Paoloni, E. A. Weiber, Z. H. Jiang and P. Jannasch, *Macromolecules*, 2012, 45, 1447-1459.
28. T. B. Norsten, M. D. Guiver, J. Murphy, T. Astill, T. Navessin, S. Holdcroft, B. L. Frankamp, V. M. Rotello and J. F. Ding, *Advanced Functional Materials*, 2006, 16, 1814-1822.

29. J. F. Blachot, O. Diat, J. L. Putaux, A. L. Rollet, L. Rubatat, C. Vallois, M. Muller and G. Gebel, *Journal of Membrane Science*, 2003, 214, 31-42.
30. C. Genies, R. Mercier, B. Sillion, N. Cornet, G. Gebel and M. Pineri, *Polymer*, 2001, 42, 359-373.
31. A. L. Rollet, G. Gebel, J. P. Simonin and P. Turq, *Journal of Polymer Science Part B-Polymer Physics*, 2001, 39, 548-558.
32. B. Guilleaume, J. Blaul, M. Ballauff, M. Wittemann, M. Rehahn and G. Goerigk, *European Physical Journal E*, 2002, 8, 299-309.
33. H. Allen, D. G. Watson, L. Brammer, A. G. Orpen and R. Taylor, *Typical interatomic distances: organic compounds. International tables for crystallography*, 2006.
34. S. M. J. Zaidi, S. D. Mikhailenko, G. P. Robertson, M. D. Guiver and S. Kaliaguine, *Journal of Membrane Science*, 2000, 173, 17-34.
35. G. Gebel, P. Aldebert and M. Pineri, *Macromolecules*, 1987, 20, 1425-1428.
36. L. A. S. D. Prado, H. Wittich, K. Schulte, G. Goerigk, V. M. Garamus, R. Willumeit, S. Vetter, B. Ruffmann and S. P. Nunes, *Journal of Polymer Science Part B-Polymer Physics*, 2004, 42, 567-575.
37. S. Min and D. Kim, *Solid State Ionics*, 2010, 180, 1690-1693.
38. B. Yang and A. Manthiram, *Journal of Power Sources*, 2006, 153, 29-35.
39. M. T. Bishop, F. E. Karasz, P. S. Russo and K. H. Langley, *Macromolecules*, 1985, 18, 86-93.
40. H. Mendil-Jakani, P. M. Legrand, V. H. Mareau, A. Morin and L. Gonon, *Proc. SSPC16 Conf., Grenoble* 2012, 163.